Inclusive Scattering from Nuclei at $x > 1$ and High Q^2 with a 6 GeV Beam

B.W. Filippone (Spokesperson), C.E. Jones, E.M. Hughes, R.D. McKeown
California Institute of Technology

C. Armstrong, R. Carlini, R. Ent, K. Garrow, A. Lung (Spokesperson),
D. Mack, J. Mitchell, S. Wood, W. Vulcan, C. Yan
Thomas Jefferson National Accelerator Facility

J. Arrington
Argonne National Laboratory

O.K. Baker, L. Gan, C.E. Keppel, L. Tang
Hampton University

R. Milner
Massachusetts Institute of Technology

J. Jourdan, A. Honegger, M. Muehlbauer, T. Petitjean, D. Rohe, I. Sick, G. Warren
University of Basel

D.B. Day (Spokesperson), R.L. Lindgren, R. Minehart, Y. Prok,
O. Rondon-Aramayo, M. Zeier, B. Zihlmann
University of Virginia
(December 17, 1998)

We propose an extension to Jefferson Lab Experiment 89-008, an inclusive electron-nucleus scattering experiment in the domain of large x and Q^2. Additional measurements with a 6 GeV beam would allow study of the scaling behavior at large Q^2 and provide important constraints on the components of the nuclear wave function at large momentum and removal energy. Measurements with few-body nuclei (^{2}H and ^{3}He) and a range of heavy nuclei (C, Fe, and Au) allow contact with theoretical calculations via essentially "exact" calculations for few-body systems and extrapolation of the heavier systems to potentially calculable nuclear matter.

I. INTRODUCTION

The physics motivation for this proposed extension is similar to that of the original proposal (89-008), but with some new components that are the result of several recent analyses and theoretical studies. These are discussed in the following sections. We then discuss the results from experiment 89-008 with a 4 GeV beam, followed by a presentation of new physics possibilities accessible with a 6 GeV beam.

This proposal requests time to make inclusive electron scattering measurements with several few-body nuclei and several heavy nuclei at high momentum transfers. The measurements with few-body nuclei allow comparisons with essentially exact calculations of nuclear wave functions and provide an important complement to the semi-inclusive (e,e′p) measurements already approved. The measurements with heavy nuclei should allow extrapolation to nuclear matter where again rigorous calculations can be performed and compared to the data.

A. Connection to Deep Inelastic Scattering (DIS)

The response of the nucleus in the range $x > 1$ is expected to be composed of both deep-inelastic scattering from quarks in the nucleus and elastic scattering from the bound nucleons (quasielastic). For both the bound quark and bound nucleon cases it is the non-zero momentum of the bound nucleons that permits scattering into a kinematic region that is forbidden for the free nucleon. The scattering from quarks should exhibit scaling in the Bjorken x variable (experimentally verified for $x < 1$), while the scattering from the nucleons exhibits y scaling (discussed below). However the respective scaling functions for the two processes appear to be dramatically different. It is the inclusive structure functions (eg. νW_2^A) that scale for the quark case while for the nucleon case it is the cross section weighted by the elastic form factors [$G_E(Q^2)$ and $G_M(Q^2)$] that exhibit scaling. In a simple impulse approximation (Quark-Parton model for quark scattering, quasielastic nucleon scattering for the nucleon scattering) the DIS scaling functions are related to the *quark* momentum distributions in the nucleus, while the quasi-elastic scaling function is related to the *nucleon* momentum distributions. It is the weighting by the elastic form factors, which fall with a high power of Q^2, that causes the quasielastic response to vanish in the limit of $Q^2 = \infty$. In this limit the deep inelastic scattering from quarks should dominate the response for $x > 1$. Thus the two types of scaling appear to be significantly different. A possible connection between the two has been suggested in several analyses of the previous data [1–4]. Here the nuclear structure function is analyzed vs the Nachtmann scaling variable ξ, and an interesting scaling (for all x) is suggested by the data [4] (see Fig. 1). The Q^2 range of the previous SLAC data was too limited to draw firm conclusions about the nature of this scaling. In fact one theoretical analysis [5] suggests that the observed scaling is accidental and will break down at larger Q^2.

Exploring the transition from y scaling to x scaling requires measurements at the highest possible Q^2. Measurements with a 6 GeV beam will significantly extend the accessible Q^2 range (up to 70%) compared to what is possible with a 4 GeV beam. Comparisons of ^{2}H and heavy nuclei at $x > 1$ for high Q^2 permit searches for modifications of quark distributions due to the nuclear medium in a new kinematic regime.

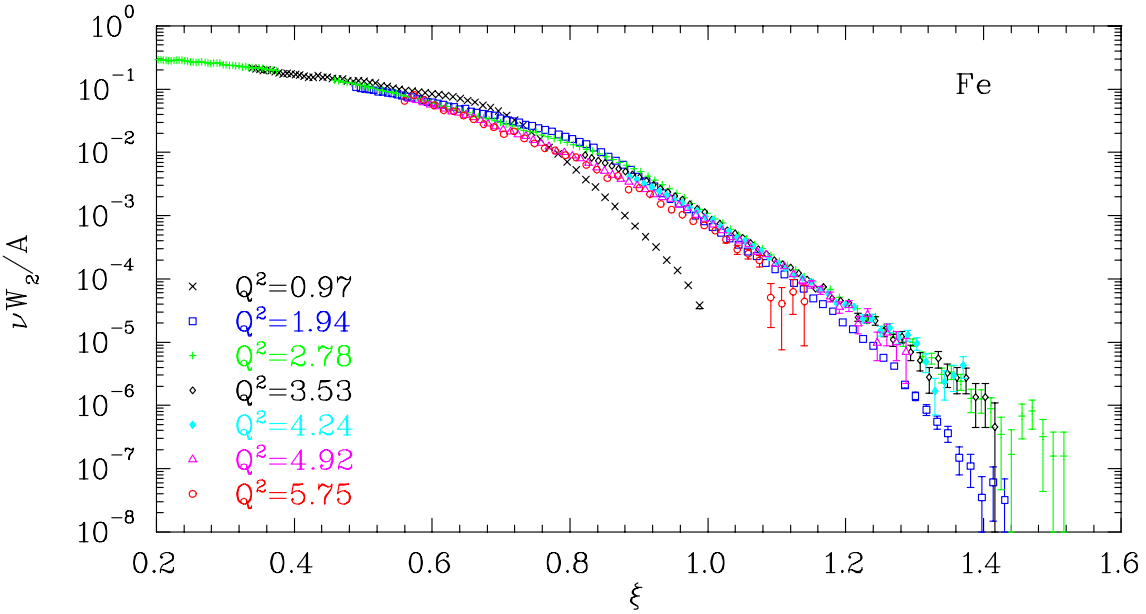

FIG. 1. Structure function per nucleon for Fe vs. the Nachtmann scaling variable from Jefferson Lab E89-008. The Q^2 values are given for Bjorken $x = 1$. Errors shown are statistical only.

B. High Momentum Components in the Nucleus

High energy electron scattering from nuclei can provide important information on the wave function of nucleons in the nucleus. In particular, with simple assumptions about the reaction mechanism, scaling functions can be deduced that, if shown to scale (i.e. are independent of length scale or momentum transfer), can provide information about the momentum and energy distribution of nucleons in a nucleus. Several theoretical studies [6–9] have indicated that such measurements may provide direct access to short-range nucleon-nucleon correlations.

The concept of y-scaling in electron-nucleus scattering was first introduced by West [10] and Kawazoe *et al.* [11]. They showed that in the impulse approximation, if quasielastic scattering from a nucleon in the nucleus was the dominant reaction mechanism, a scaling function $F(y)$ could be extracted from the measured cross section which was related to the momentum distribution of the nucleons in the nucleus. In the simplest approximation the corresponding scaling variable y is the minimum momentum of the struck nucleon along the direction of the virtual photon.

The scaling function is defined as the ratio of the measured cross section to the off-shell electron-nucleon cross section multiplied by a kinematic factor:

$$F(y) = \frac{d^2\sigma}{d\Omega d\nu}[Z\sigma_p + N\sigma_n]^{-1}\frac{q}{(M^2 + (y+q)^2)^{\frac{1}{2}}}$$

where Z and N are the number of protons and neutrons in the target nucleus, the off-shell cross sections σ_p and σ_n are taken from σ_{CC1} from Ref. [12] using the elastic form factors from Ref. [13], q is the three-momentum transfer and M is the mass of the proton. The y variable is defined through the equation [14]:

$$\nu + M_A = (M^2 + q^2 + y^2 + 2yq)^{\frac{1}{2}} + (M_{A-1}^2 + y^2)^{\frac{1}{2}}$$

where M_A is the mass of the target nucleus and M_{A-1} is the ground state mass of the $A-1$ nucleus.

In general, within the impulse approximation, the scaling function depends on both y and momentum transfer - $F(y, Q^2)$ - but at sufficiently high Q^2 the dependence on Q^2 should vanish yielding scaling. However the simple impulse approximation picture breaks down when the final-state interactions (FSI) of the struck nucleon with the rest of the nucleus are included. Previous calculations [15–22] suggest that the contributions from final state interactions should vanish at sufficiently high Q^2. The scaling function for Fe extracted from experiment 89-008 is shown in Fig. 2. These data suggest, for the first time, that there is an approach to a scaling limit for heavy nuclei at large $-y$ for $Q^2 > 3$ GeV/c^2. This is shown in Fig. 3 for data from 89-008 where the Q^2 variation of $F(y)$ for several fixed values

of y is shown. Note that the cross section (see Section II.A. and Fig. 4) varies over many orders of magnitude for the Q^2 range shown in the figure.

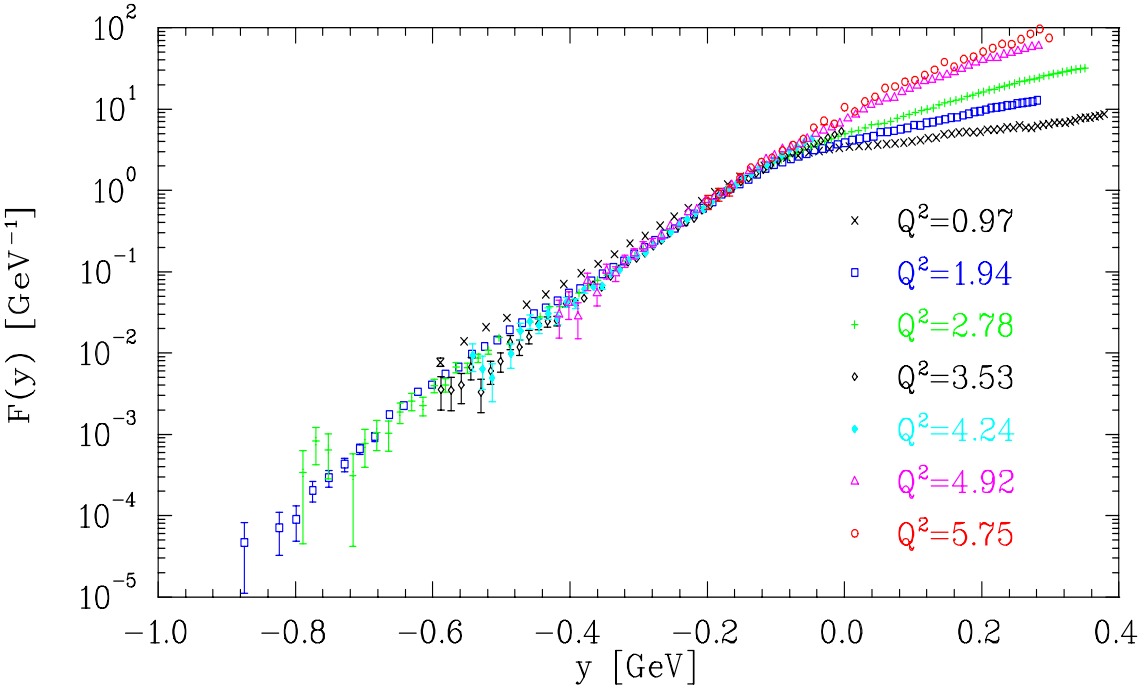

FIG. 2. Scaling function $F(y)$ for Fe from E89-008. The Q^2 values are given for Bjorken $x = 1$.

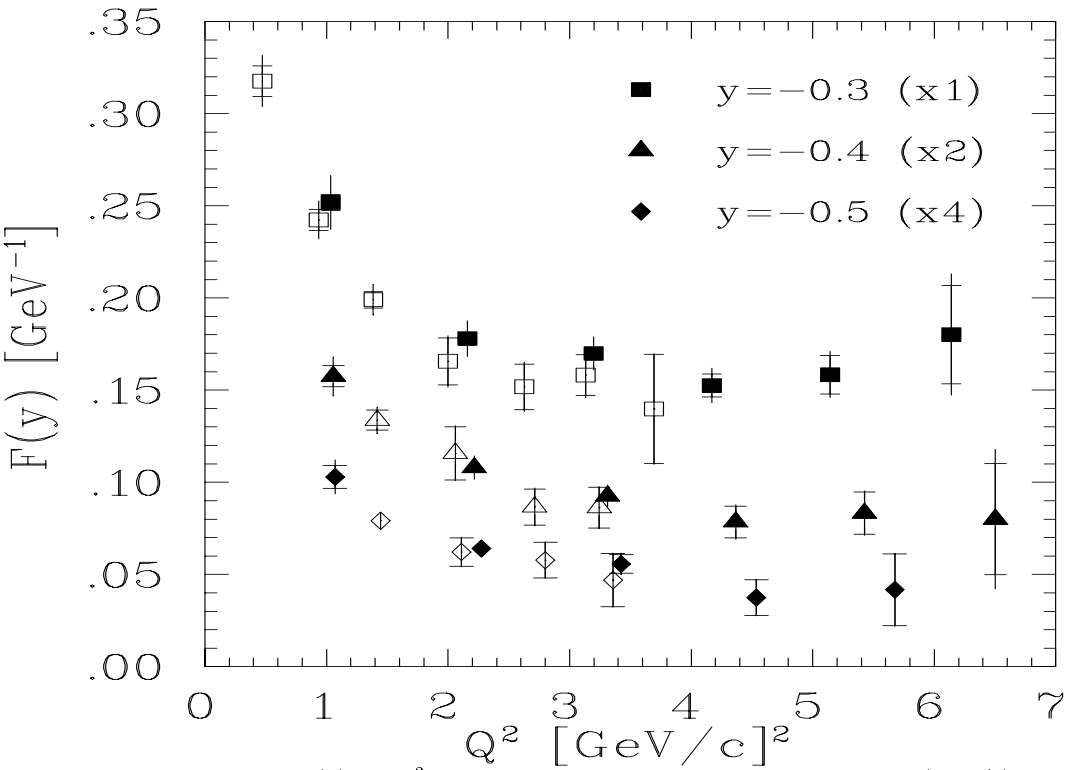

FIG. 3. Scaling function $F(y)$ vs. Q^2 for Fe for fixed values of $y = -0.3, -0.4, -0.5$ (GeV/c). The open points are calculated from the measured cross sections of the SLAC NE3 experiment see (Ref. 4). The scaling function for each value of y has been multiplied by the factors noted in parentheses.

While the approach to a scaling limit is suggestive of an approach to the impulse approximation limit, it is not definitive. Several recent calculations [23,24] have pointed out that the FSI of a struck nucleon with the mean field of the rest of the nucleus is a rapidly decreasing function of Q^2. But FSI of the struck nucleon with a correlated, high-momentum nucleon may show a very weak Q^2 dependence. Experimental measurements at higher Q^2 are essential in allowing an understanding of the role of FSI in inclusive scattering. The "holy grail" of these studies is to correct or eliminate FSI so that by using the impulse approximation, the nuclear spectral function $S(p, E)$ at high values of p and E can be extracted. The region of high p includes the highly interesting regime of short-range correlations that are expected to be present within nuclei. As both the impulse approximation strength and the high Q^2 FSI discussed above are dominated by short-range nucleon-nucleon interactions, improved data at higher Q^2 may allow direct access to this interesting many-body phenomenon.

II. JEFFERSON LAB MEASUREMENTS

A. Results from 4 GeV Running

CEBAF offers the possibility of significant improvement over previous experiments. The solid angle of the HMS as well as it's large momentum acceptance allows measurements in previously unexplored regions of x and Q^2. A program of measurements with 4 GeV beam ran in Hall C in Summer 1996, and greatly increased the x range of the available data for $1 < Q^2 < 6$ (GeV/c)^2. Cross sections were measured at seven angles and are shown in Fig. 4. Data was taken on C, Fe, and Au as well as liquid targets of hydrogen and deuterium. Scattered electrons were detected in the HMS and SOS spectrometers using their standard detector packages.

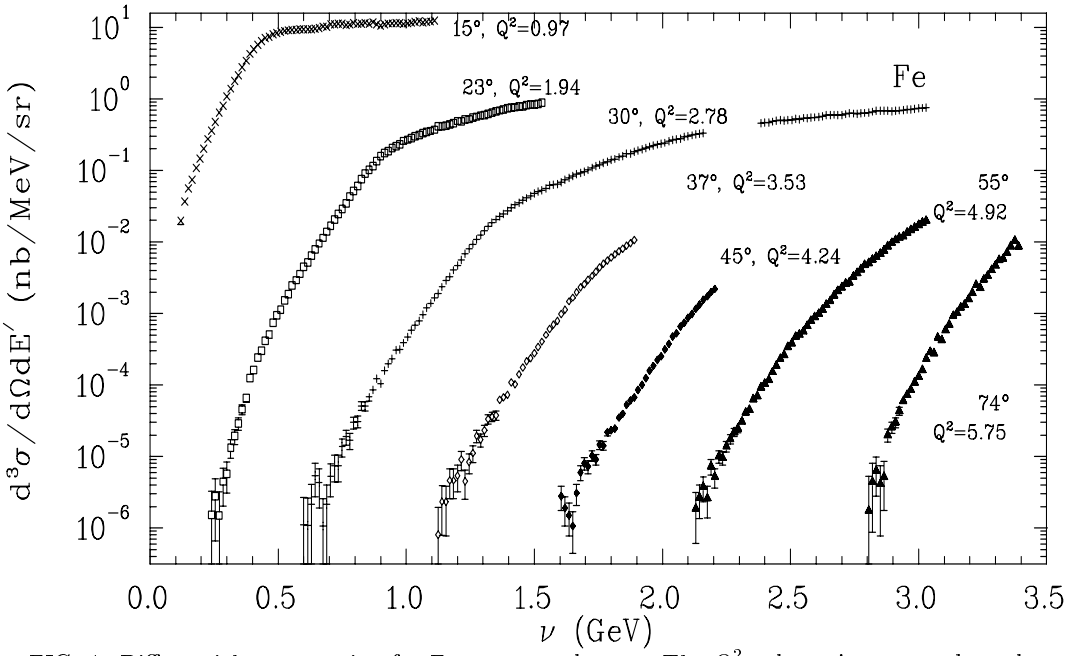

FIG. 4. Differential cross section for Fe vs energy loss, ν. The Q^2 values given at each angle correspond to Bjorken $x = 1$. Statistical errors only are shown.

Fig. 5 shows the kinematic range in the Bjorken x variable and Q^2. The region below the dashed curve is what was measured in Experiment 89-008 using a 4 GeV CEBAF beam. Previous SLAC measurements of inclusive electron scattering from nuclei [1] were limited to $x \leq 3$ and $Q^2 \leq 3$ (GeV/c)^2. The nuclear structure function, $\nu W_2/A$, was extracted and scaling in both Bjorken x and Nachtmann ξ have been studied (see Section I.A. and Fig. 1). Also the Q^2 dependence of the structure function for fixed bins of x and ξ has been studied. A draft of an article for PRL on the results for the nuclear structure function is in preparation.

Fig. 6 shows the kinematic range in the scaling variable y and Q^2. Again, the area below the dashed curve is what was measured in 89-008 (see Section I.B. and Figs. 2 and 3). An article has been submitted to Physical Review

Letters describing the inclusive scattering measurement and the analysis in terms of the y scaling variable [25]. A copy of the article is included in this proposal as Appendix A.

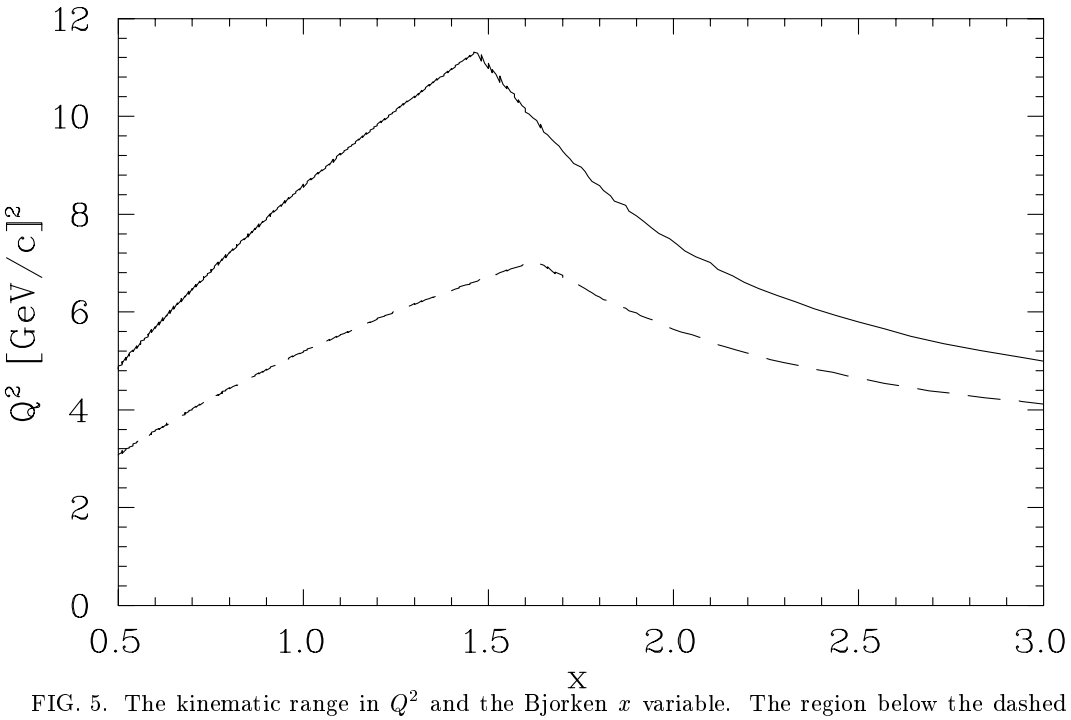

FIG. 5. The kinematic range in Q^2 and the Bjorken x variable. The region below the dashed curve is the range of data measured in E89-008 using a 4 GeV CEBAF beam. The region between the solid curve and the dashed curve indicates the increased range possible with a 6 GeV beam.

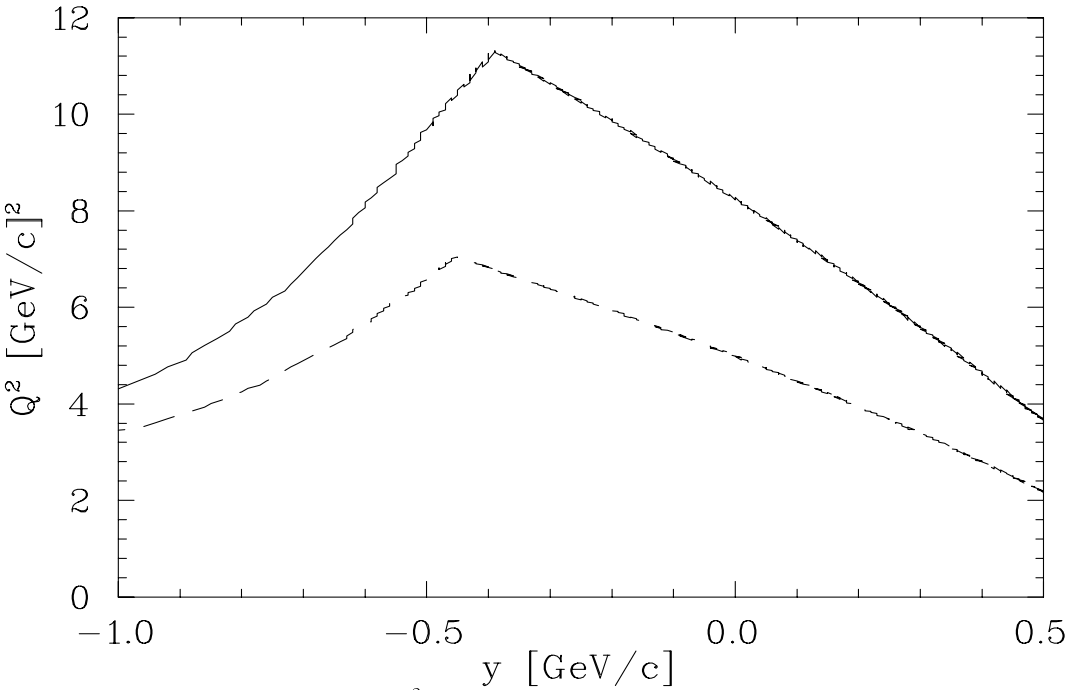

FIG. 6. The kinematic range in Q^2 and the scaling variable y. The region below the dashed curve is the range of data measured in E89-008 using a 4 GeV CEBAF beam. The region between the solid curve and the dashed curve indicates the increased range possible with a 6 GeV beam.

B. Backgrounds and Systematic Errors

We have learned a great deal from the 4 GeV running about how to improve the measurement, particularly in determining backgrounds. One source of background is the pions in the detector hut which contaminate your electron distribution. During E89-008 this contamination was always less than 1% in the HMS when using the calorimeter and Cerenkov information for particle identification. It is estimated that during 6 GeV running this pion contamination will get somewhat worse, but is still expected to be negligible. In the event that it is non-negligible we can include prescaled pions in our trigger to measure the contamination. Also since the 4 GeV running was completed, several layers of the HMS calorimeter have been outfitted with phototubes on both ends of each lead glass block. This will improve our ability to distinguish electrons from pions.

There is also a background from secondary electrons produced in the target which was larger than expected for E89-008. The main source likely comes from electro-production and photo-production of neutral pions. These pions then decay into photons which can produce positron-electron pairs. This background is charge-symmetric, and can be measured directly by changing the spectrometer to positive polarity and detecting the produced positrons. For the largest angles measured in E89-008 (55° and 74°), this background was significant and required a fit to our positron measurements and subtraction from our electron data (see Ref. [4] for more details). As a result, we have decided to limit our running with a 6 GeV beam to 60°, and have included time in our beamtime request to measure this background.

The combined systematic uncertainties from the E89-008 run totalled 3.2 to 4.7% for the HMS data with the primary contributors being knowledge of the acceptance, radiative corrections, target thickness, and bin centering (correcting an integral number of counts within a momentum/angle bin to the measured cross section at the center of the bin). Each of these four items ranged from approximately 1% to 2% depending on the scattering angle. Table 1 below from Ref. [4] summarizes the systematic uncertainties during the 4 GeV running. We expect similar results for the 6 GeV running.

TABLE I. Systematic uncertainties in the extraction of the cross section for 4 GeV running. Entries with an asterisk indicate that a correction was made directly to the cross section which had the listed uncertainty. Entries without an asterisk indicate no correction to the cross section, just a contribution to the overall uncertainty.

Systematic	HMS
Acceptance Correction	1.0-2.2%*
Radiative Correction	2.5%*
Target Track Cuts	0.5%
Bin Centering Correction	1.0-2.2%*
PID Efficiency	0.5%*
Charge Measurement	1.0%
Target Thickness	0.5-2.0%
Target/Beam Position Offset	0.25%
Tracking Efficiency	0.5%*
Trigger Efficiency	0.05%*
Normalization	0.0%
COMBINED UNCERTAINTY	3.2-4.7%

C. Proposed Measurements with 6 GeV Running

An increase in beam energy to 6 GeV would have the greatest impact on the Q^2 range for kinematic points with $x < 1.6$. For example, at $x = 1.4$ the Q^2 range would increase by 70% from 6.5 to 11.0 (GeV/c)^2. This is shown in Fig. 5 where the region between the solid curve and the dashed curve indicates the increase in achievable kinematic range with a 6 GeV beam. This extended Q^2 data is critical to studies of the transition from scattering from nucleons to scattering from quarks as described in the introduction.

This corresponds to a significant increase in the Q^2 range accessible for large negative values of y (see Fig. 6) allowing direct study of the approach to the scaling limit. For example at $y = -0.3$ the Q^2 limit increases from 6 to almost 10.5 (GeV/c)^2 just with the increase in beam energy. Correspondingly for $y = -0.4$ it increases from 5.5 to 11.0 (GeV/c)^2.

An addition to the measurement since the original proposal in 1994 is the inclusion of a ^{3}He cryotarget. The proposed data would increase the measured Q^2 coverage for ^{3}He by nearly a factor of 3 from 3.5 (GeV/c)^2 in the early SLAC data up to approximately 10 (GeV/c)^2.

III. EXPERIMENTAL EQUIPMENT

The experimental set-up for measurements with a 6 GeV beam would be essentially the same as used for the 4 GeV measurements. No new detectors would be needed. Data would be taken in the HMS spectrometer using a detector package including a threshold gas Cerenkov counter and a lead glass shower counter for rejection of pion background. Several nuclear targets (eg. ^{12}C, ^{56}Fe, and ^{197}Au) would be used as well as cryogenic targets.

A cryogenic hydrogen target is necessary for calibration and a cryogenic deuterium target for production data. These are currently part of the standard Hall C cryotarget system. Our understanding is that by the end of the 1999 calendar year a ^{3}He cell will also be available as part of the Hall C target loops.

The measurements would be done at several angles to cover the full kinematic range. Table II is a list of estimated running times for five angle settings between $\theta = 20^\circ$ and 60°. The assumptions are 60 μA of beam current, a spectrometer solid angle of 7 msr, a momentum bite of 16%, a fixed x bin of 0.05, and a maximum statistical error of 8%.

IV. REQUEST TO LABORATORY

We request approval to extend the measurements of inclusive scattering from nuclei at $x > 1$ and high Q^2 with a 6 GeV beam at Jefferson Lab. The summed run time at five angles for each solid target is 60 hours (times three targets totals 180 hours). The summed run time at five angles for each cryotarget is 90 hours (times two targets totals 180 hours).

Check-out and commissioning time is estimated to require 25 hours, hydrogen elastic running an additional 25 hours, and cross calibration to E89-008 with a 4 GeV beam also requires approximately 25 hours. Special runs to measure backgrounds (positron background and empty target runs) will require approximately 50 hours. This sums to a total time for check-out, calibration, and background measurements of 125 hours.

The average overhead for configuration changes will vary from approximately 30 minutes to 1 hour depending on the target changes involved and whether the magnet polarity will be changed. We estimate a total of 100 hours of overhead time for configuration changes.

We request measurements on three nuclear targets, as well as hydrogen, deuterium, and ^{3}He, for a total beam time request of 585 hours, or 25 beam days.

TABLE II. Kinematics of the proposed experiment for 6 GeV running.

θ (deg)	E' (GeV)	x_{range}	y_{range} (GeV/c)	Q^2_{range} (GeV/c)^2	time(hrs) C,Fe,Au	time(hrs) D,^{3}He
20.0	3.5-5.3	0.5-2.9	-0.8-0.3	2.5-3.8	6	9
30.0	2.2-4.1	0.5-1.8	-0.6-0.4	3.5-6.6	11	16
40.0	1.4-3.0	0.5-1.5	-0.4-0.4	4.0-8.5	14	21
50.0	1.0-2.1	0.5-1.3	-0.2-0.4	4.4-9.2	14	21
60.0	0.8-1.8	0.5-1.3	-0.3-0.4	4.5-10.6	15	23

[1] D. B. Day *et al.*, Phys. Rev. Lett. **59**, 427 (1987).
[2] B. W. Filippone *et al.*, Phys. Rev. **C45**, 1582 (1992).
[3] J. Arrington *et al.* Phys. Rev. **C53**, 2248 (1996).
[4] J. Arrington PhD Thesis, unpublished. URL address: http://www.krl.caltech.edu/johna/thesis, (1998).
[5] O. Benhar and S. Liuti, Phys. Lett. **B358**, 173 (1995).
[6] D. Day *et al.* Ann. Rev. Nucl. Part. Sci. **40**, 357 (1990).
[7] L. L. Frankfurt *et al.*, Phys. Rev. **C48**, 2451 (1993).
[8] C. C. degli Atti and S. Simula, Phys. Lett. **B325**, 276 (1994).
[9] O. Benhar *et al.*, Phys. Lett. **B343**, 47 (1995).
[10] G. B. West, Phys. Rep. **18**, 263 (1975).
[11] Y. Kawazoe, G. Takeda and H. Matsuzaki, Prog. Theo. Phys. **54**, 1394 (1975).
[12] T. DeForest, Nucl. Phys. **A392**, 232 (1983).
[13] M. Gari and W. Krümpelmann, Phys. Lett. **B141**, 295 (1984).
[14] E. Pace and G. Salmé, Phys. Lett. **B110**, 411 (1982).
[15] B. L. Ioffe, V. Khoze, and L. N. Lipatov, **Hard Processes** (Horth-Holland, Amsterdam, 1984).
[16] E. Pace, G. Salmé, and G. B. West, Phys. Lett. **B273**, 205 (1991).
[17] O. Benhar *et al.*, Phys. Rev. **C44**, 2328 (1991).
[18] O. Greenberg, Phys. Rev. **D47**, 331 (1993).
[19] B. L. Ioffe, ZhEFT Lett. **58**, 930 (1993).
[20] E. Pace, G. Salmé, and A. S. Rinat, Nucl. Phys. **A572**, 1 (1993).
[21] S. A. Gurvitz and A. S. Rinat, Phys. Rev. **C47**, 2901 (1993).
[22] A. S. Rinat and M. F. Taragin, Nucl. Phys. **A620**, 417 (1997). Erratum: Nucl. Phys. **A624**, 773 (1997).
[23] S. Simula, Private Communication (1998).
[24] O. Benhar, Private Communication (1998).
[25] J. Arrington *et al.*, "Inclusive Electron–Nucleus Scattering at Large Momentum Transfer", submitted to PRL in November 1998.

V. APPENDIX A: ARTICLE SUBMITTED TO PRL FROM E89-008 COLLABORATION.

Inclusive Electron-Nucleus Scattering at Large Momentum Transfer

J. Arrington[2*], C. S. Armstrong[11#], T. Averett[2+], O. K. Baker[4,9], L. de Bever[1], C. W. Bochna[5], W. Boeglin[3], B. Bray[2], R. D. Carlini[9], G. Collins[6], C. Cothran[10], D. Crabb[10], D. Day[10], J. A. Dunne[9], D. Dutta[7], R. Ent[9], B. W. Filippone[2], A. Honegger[1], E. W. Hughes[2], J. Jensen[2], J. Jourdan[1], C. E. Keppel[4,9], D. M. Koltenuk[8], R. Lindgren[10], A. Lung[6], D. J Mack[9], J. McCarthy[10], R. D. McKeown[2], D. Meekins[11], J. H. Mitchell[9], H. G. Mkrtchyan[9], G. Niculescu[4], I. Niculescu[4], T. Petitjean[1], O. Rondon[10], I. Sick[1], C. Smith[10], B. Terburg[5] W. F. Vulcan[9], S. A. Wood[9], C. Yan[9], J. Zhao[1], B. Zihlmann[10]

[1] *University of Basel, Basel Switzerland*

[2] *Kellogg Radiation Laboratory, California Institute of Technology, Pasadena CA 91125*

[3] *Florida International University, University Park FL 33199*

[4] *Hampton University, Hampton VA 23668*

[5] *University of Illinois, Urbana-Champaign IL 61801*

[6] *University of Maryland, College Park MD 20742*

[7] *Northwestern University, Evanston IL 60201*

[8] *University of Pennsylvania, Philadelphia PA 19104*

[9] *Thomas Jefferson National Accelerator Facility, Newport News VA 23606*

[10] *University of Virginia, Charlottesville VA 22901*

[11] *College of William and Mary, Williamsburg, VA 23187*

(Aug. 15, 1998)

Abstract: Inclusive electron scattering is measured with 4.045 GeV incident beam energy from C, Fe and Au targets. The measured energy transfers and angles correspond to a kinematic range for Bjorken $x > 1$ and momentum transfers from $Q^2 = 1 - 7$ (GeV/c)^2. When analyzed in terms of the y-scaling function the data show for the first time an approach to scaling for values of the initial nucleon momenta significantly greater than the nuclear matter Fermi-momentum (i.e. > 0.3 GeV/c).

PACS numbers: 25.30.Fj, 13.60.Hb

High energy electron scattering from nuclei can provide important information on the wave function of nucleons in the nucleus.. In particular, with simple assumptions about the reaction mechanism, scaling functions can be deduced that, if shown to scale (i.e. are independent of length scale or momentum transfer), can provide information about the momentum and energy distribution of nucleons in a nucleus. Several theoretical studies [1–4] have indicated that such measurements may provide direct access to short-range nucleon-nucleon correlations.

The concept of y-scaling in electron-nucleus scattering was first introduced by West [5] and Kawazoe citekawa. He showed that in the impulse approximation, if quasielastic scattering from a nucleon in the nucleus was the dominant reaction mechanism, a scaling function $F(y)$ could be extracted from the measured cross section which was related to the momentum distribution of the nucleons in the nucleus. The corresponding scaling variable y in the simplest approximation is the minimum momentum of the struck nucleon along the direction of the virtual photon. In general the scaling function depends on both y and momentum transfer - $F(y, Q^2)$ - but at sufficiently high Q^2 ($-Q^2$ is the square of the four-momentum transfer) the dependence on Q^2 should vanish yielding scaling. However the simple impulse approximation picture breaks down when the final-state interactions (FSI) of the struck nucleon with the rest of the nucleus are included. Previous calculations [7–14] suggest that the contributions from final state interactions should vanish at sufficiently high Q^2. A previous SLAC measurement [15] suggested an approach to the scaling limit for heavy nuclei but only for low values of $|y| < 0.3$ GeV/c at momentum transfers up to 3 (GeV/c)^2. The data presented here represents a significant increase in the Q^2 range compared to previous mesurements while also extending the coverage in y.

The present data was obtained in Hall C at the Jefferson Laboratory, using 4.045 GeV electron beams with intensities from 10 - 80 μA. The absolute beam energy was calibrated to 0.03% using 0.8 GeV elastic scattering from carbon and BeO targets and 4.0 GeV elastic scattering from hydrogen. The beam current was monitored with three calibrated resonant cavities. The beam energy resolution was better than 0.05% as defined by the accelerator acceptance. Solid targets of C (nominally 2% and 6% of a radiation length), Fe (nominally 1.5% and 6% of a radiation length) and Au (nominally 6% of a radiation length) with natural isotopic abundance were used. Data was also taken with liquid targets of hydrogen and deuterium (nominally 4 and 15 cm in length). Scattering from hydrogen allows a cross check of the absolute normalization of the cross section; results from the deuterium target will be presented elsewhere. Less than 1% density variations were observed for the liquid targets due to beam heating for incident beam currents up to 55 μA (maximum current used for the liquid targets) when

the 200 μm $\times$ 200 μm beam was rastered by a pair of electro-magnets to the typical spot-size of $\pm$ 1.2 mm.

The scattered electrons were detected with the High Momentum Spectrometer (HMS) at angles of $15^\circ, 23^\circ, 30^\circ, 37^\circ, 45^\circ$ and 55° and the Short Orbit Spectrometer (SOS) at an angle of 74°. Both spectrometers took data simultaneously in singles mode with nearly identical detector systems configured for electron detection. Each detector system included two planes of plastic scintillator for triggering, two six-element drift chambers for tracking information as well as a gas Cerenkov detector and Pb glass calorimeter for particle identification.

The measured tracks were required to reconstruct to the target location. For the HMS, additional cuts were applied to eliminate events produced on the pole pieces of the spectrometer magnets. Cuts were also applied to select electrons and reject π^- using the signals from the Cerenkov detector and Calorimeter. The combined efficiency of all the cuts was $> 98\%$. The binned events were corrected for spectrometer acceptance using an acceptance function generated by a Monte Carlo calculation [16] that included all apertures within the spectrometer. This calculation accurately reproduced the distributions and cross section from hydrogen elastic scattering. Estimated systematic uncertainties due to the acceptance are $< 2.5\%$. Tracking efficiencies were typically 94% - 97%. Background from mis-identified π^- was negligible for the HMS and $< 3\%$ in the worst case for the SOS. High energy photons produced principally from π^0 decay can result in secondary electrons following pair production by the photons in the target material. This background, estimated by measuring positron yields with the spectrometer magnetic fields reversed, was negligible for spectrometer angles $< 55^\circ$, but was 3 - 10% at 55° and 20 - 100% at 74°. The larger values for the contribution of this background are for the 6% radiation length targets and give an estimated systematic error of 5 - 10%. However, because the large backgrounds are only present in kinematic regions where the cross section is very small, the statistical uncertainties dominate the total uncertainty.

Because of the large acceptance of the spectrometers (> 6 msr) and the rapid variation of the cross section with θ, there can be a significant variation of the cross section over the acceptance. In order to extract cross sections vs. energy transfer ν at fixed scattering angle a bin centering correction must be applied. This is accomplished with a model of the cross section [16] that is constrained to reproduce the angle and energy transfer dependence of the measurements. The cross section model was also used to apply radiative corrections using the iterative technique of Refs. [17] and [18]. Variations in the form of the model were used to estimate systematic uncertainties in these corrections. The total estimated systematic uncertainties in the bin-centering and radiative corrections were 1-2% and 2.5% respectively. Lastly a Coulomb correction was applied for the change in the incident and scattered energy due to the Coulomb acceleration from the nuclear charge. This correction was significant ($\sim 10\%$ for Fe and $\sim 20\%$ for Au) for the largest scattering angles of the present experiment.

Fig. 1 shows the measured cross sections vs. energy loss ν for Fe, where for each angle the Q^2 value at Bjorken $x = Q^2/2M\nu = 1$ is given (this value corresponds to elastic scattering from a free nucleon). Because of the significant smearing due to the Fermi motion and the large contribution from other inelastic processes (eg. π production, resonance production and deep inelastic scattering) at these relatively high Q^2, there is little evidence of a quasielastic peak. In fact the sharp bend in the spectrum at $\theta = 15^\circ$ is the only distinctive feature resulting from quasielastic scattering. At larger angles the additional inelastic processes cause even this feature to disappear. It should be noted however that quasielastic scattering is still expected to contribute significantly to the cross section for $\nu < Q^2/2M$. The minimum measured cross sections were limited by count rate and represent a factor of > 100 improvement in sensitivity compared to the previous experiment [15]. This improvement is largely due to the higher beam currents and larger acceptance spectrometers available at Jefferson Lab.

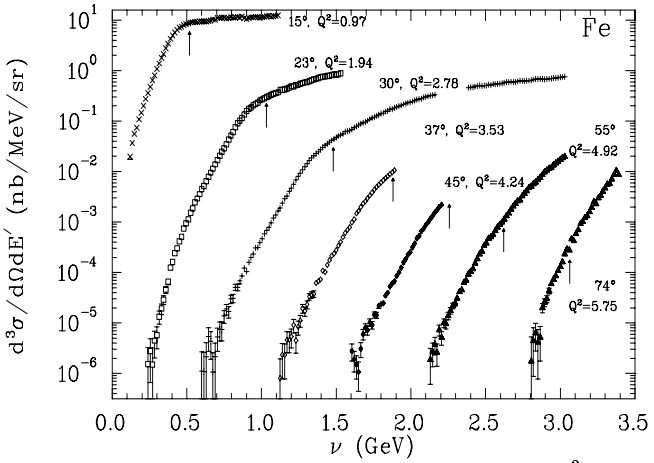

FIG. 1. Differential cross section for Fe. The Q^2 values given at each angle correspond to Bjorken $x = 1$. The value of ν for $x = 1$ is shown by an arrow for each kinematic setting. Statistical errors only are shown.

The scaling function is defined as the ratio of the measured cross section to the off-shell electron-nucleon cross section multiplied by a kinematic factor:

$$F(y) = \frac{d^2\sigma}{d\Omega d\nu}[Z\sigma_p + N\sigma_n]^{-1}\frac{q}{(M^2 + (y+q)^2)^{\frac{1}{2}}}$$

Where Z and N are the number of protons and neutrons in the target nucleus, The off-shell cross sections σ_p and σ_n are taken from σ_{CC1} from Ref. [19] using the elastic form factors from Ref. [20] q is the three-momentum transfer and M is the mass of the proton.

The y variable is defined through the equation [21]:

$$\nu + M_A = (M^2 + q^2 + y^2 + 2yq)^{\frac{1}{2}} + (M_{A-1}^2 + y^2)^{\frac{1}{2}}$$

where M_A is the mass of the target nucleus and M_{A-1} is the ground state mass of the $A-1$ nucleus.

The scaling function for Fe is shown in Fig. 2 for all measured angles. While the cross section as a function of Q^2 and ν varies over many orders of magnitude (see Fig. 1), the scaling function for values of $y < -0.1$ GeV/c shows a clear approach to a universal curve where the data can be represented by a function that depends only on y. The breakdown of scaling for small values of y is due to the dominance of other inelastic processes beyond quasielastic scattering.

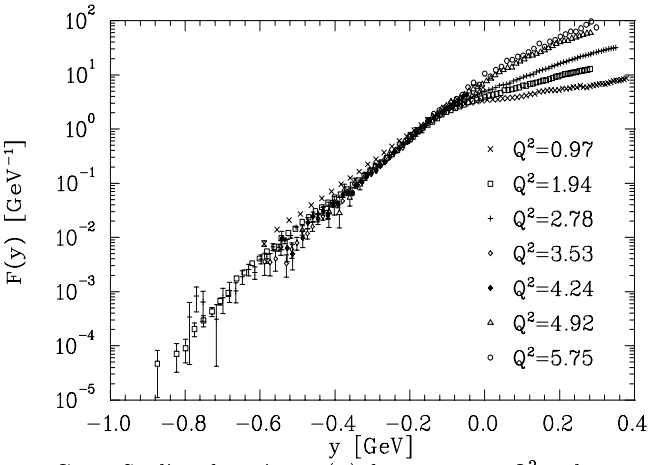

FIG. 2. Scaling function $F(y)$ for Fe. The Q^2 values are given for Bjorken $x = 1$

The approach to scaling is also shown in Figs. 3 and 4, where the Q^2 dependence of $F(y)$ at several fixed values of y is presented. For $y = -0.1$ to -0.5 GeV/c there is a clear approach to scaling as Q^2 is increased. This is the first evidence for y-scaling in heavy nuclei for $|y| > 0.3$ GeV/c.

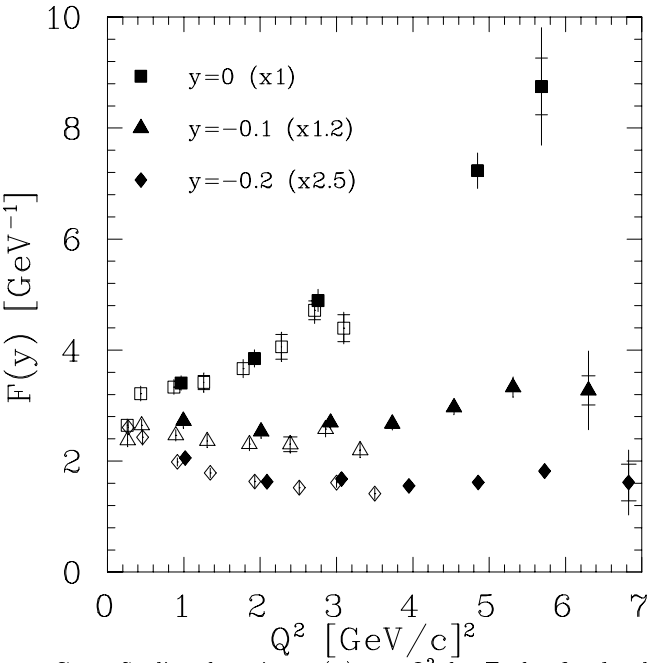

FIG. 3. Scaling function $F(y)$ vs. Q^2 for Fe for fixed values of $y = 0, -0.1, -0.2$ GeV/c. The open points are calculated from the measured cross sections of Ref. [15] including Coulomb corrections and using the definition of y as discussed in the text. The scaling functions for each value of y have been multiplied by the factors in parentheses. The inner error bar is the statistical uncertainty and the outer error bar is the statistical and systematic uncertainty added in quadrature.

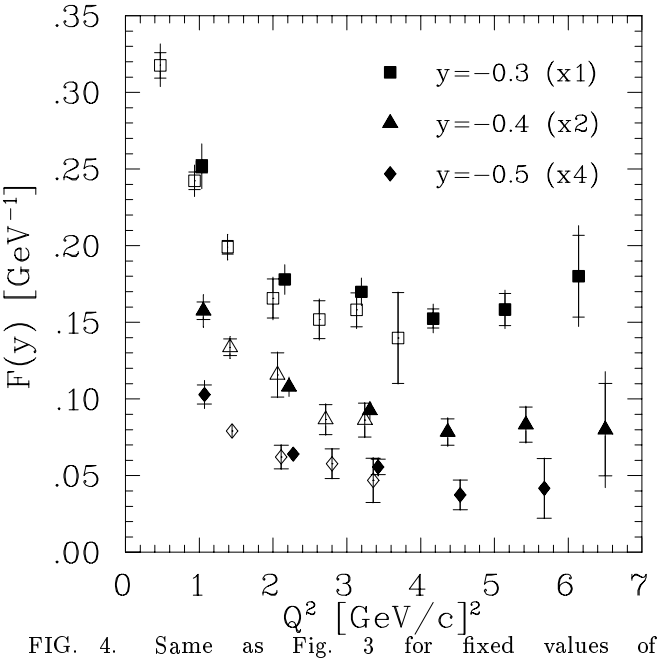

FIG. 4. Same as Fig. 3 for fixed values of $y = -0.3, -0.4, -0.5$ GeV/c.

There are, in addition, significant scaling violation observed at both low and high Q^2. The increase in $F(y)$ with Q^2 for the lowest values of y (Fig. 3) is clearly due to

the inelastic processes mentioned above. A similar effect was observed [22] previously, but only for $y \sim 0$. Calculations that include both quasielastic and other inelastic processes [9,14] indicate that at $y = 0$ these other process dominate the reaction for $Q^2 > 2$ (GeV/c)^2. At larger y (Fig. 4) there is a decrease in $F(y)$ with increasing Q^2 as the scaling is approached. This behavior contradicts the approach to scaling expected within the impulse approximation (where the scaling limit is approached from below because of incomplete kinematic coverage at low Q^2), and suggests the influence of final state interactions. A recent calculation [23] indicates that the component of the FSI resulting from the scattered nucleon interacting with the mean-field of the nucleus should be a strong decreasing function of Q^2 and becoming negligible for $Q^2 > 3$ (GeV/c)^2. An additional component in the calculation, due to interaction with a correlated nucleon, has a much weaker Q^2 dependence and may persist to the Q^2 range of the present experiment. The present data cannot distinguish between an approach to the impulse approximation scaling limit and contributions from a combination of the impulse approximation and FSI that are Q^2 independent.

Comparison of the scaling functions for C, Fe and Au show very similar distributions. This can be seen in Fig. 5 where all targets are plotted vs Q^2 for a fixed value of $y = -0.3$ GeV/c.

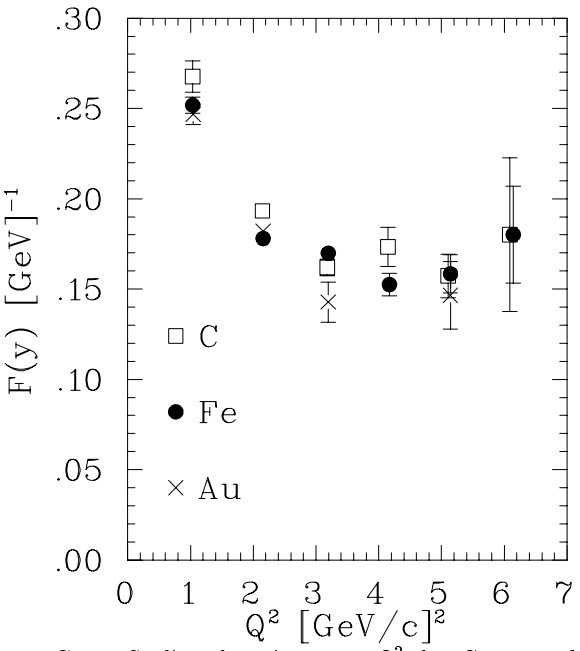

FIG. 5. Scaling function vs. Q^2 for C, Fe and Au at $y = -0.3$ GeV/c. Error bars are statistical only.

In summary, we have measured the inclusive cross section for electrons scattering from C, Fe and Au targets to $Q^2 > 6$ (GeV/c)^2, a significant increase compared to the previous experiment. When analyzed in terms of the y-scaling function the data show an approach to scaling up to $y = -0.5$ GeV/c. In this kinematic regime a scaling limit can be expected within an impulse approximation as well as from final-state interactions where both components result from a spectral function that is dominated by short-range nucleon-nucleon correlations.

We gratefully acknowledge the staff and management of Jefferson Laboratory for their efforts in delivering the electron beam. We also acknowledge helpful discussions with O. Benhar and C. Ciofi degli Atti This research was supported by the National Science Foundation, the Department of Energy and the Swiss National Science Foundation.

* Present Address: Physics Division, Argonne National Laboratory, Argonne, Il 60439.

Present Address: Thomas Jefferson National Accelerator Facility, Newport News, VA 23606.

+ Present Address: College of William and Mary, Williamsburg, VA 23187.

[1] D. Day, et al. Ann. Rev. Nucl. Part. Sci. **40**, 357 (1990).
[2] L. L. Frankfurt et al., Phys. Rev. **C48**, 2451 (1993).
[3] C. C. degli Atti and S. Simula, Phys. Lett. **B325**, 276 (1994).
[4] O. Benhar et al., Phys. Lett. **B343**, 47 (1995),
[5] G. B. West, Phys. Rep. **18**, 263 (1975).
[6] Kawazoe, Prog. Theo. Phys. **54**, 1394 (1975) G. B. West, Phys. Rep. 18, 263 (1975).
[7] B. L. Ioffe, V. Khoze, and L. N. Lipatov, **Hard Processes** (Horth-Holland, Amsterdam, 1984).
[8] E. Pace, G. Salmé, and G. B. West, Phys. Lett. **B273**, 205 (1991).
[9] O. Benhar, et al., Phys. Rev. **C44**, 2328 (1991).
[10] O. Greenberg, Phys. Rev. **D47**, 331 (1993).
[11] B. L. Ioffe, ZhEFT Lett. **58**, 930 (1993).
[12] E. Pace, G. Salmé, and A. S. Rinat, Nucl. Phys. **A572**, 1 (1993).
[13] S. A. Gurvitz and A. S. Rinat, Phys. Rev. **C47**, 2901 (1993).
[14] A. S. Rinat and M. F. Taragin, Nucl. Phys. **A620**, 417 (1997). Erratum: Nucl. Phys. **A624**, 773 (1997).
[15] D. B. Day et al., Phys. Rev. Lett. **59**, 427 (1987).
[16] J. Arrington Ph.D. Thesis, unpublished. URL address: http://www.krl.caltech.edu/~johna/thesis, (1998).
[17] S. Stein et al., Phys. Rev. **D12**, 1884 (1975).
[18] D. H. Potterveld, Ph.D. thesis, California Institute of Technology, 1989.
[19] T. DeForest, Nucl. Phys. **A392**, 232 (1983).
[20] M. Gari and W. Krümpelmann, Phys. Lett. **B141**, 295 (1984).
[21] E. Pace and G. Salmé, Phys. Lett. **B110**, 411 (1982).
[22] J. Arrington et al., Phys. Rev. **C53**, 2248 (1996).
[23] S. Simula, private communication (1998).